

# Simulation of Load Bearing Rod Rolling of Carbon-Manganese Steel Using the “Phantom Roll” Method.

P.O. Aiyedun, Ph.D.<sup>1</sup>, L.E. Oseghale, M.Sc.<sup>2</sup>, and O.J. Alamu, Ph.D.<sup>1</sup>

<sup>1</sup>Department of Mechanical Engineering, University of Agriculture, PMB 2240, Abeokuta, Nigeria.

<sup>2</sup>Mechanical Engineering Department, University of Ibadan, Ibadan, Nigeria.

E-mail: [laiyedun\\_494@yahoo.com](mailto:laiyedun_494@yahoo.com)  
[tolasum@yahoo.com](mailto:tolasum@yahoo.com)

## ABSTRACT

Rolling load for a 17 pass, 125 x 125mm carbon manganese steel billet hot rolled to a 16mm diameter rod was simulated. Load calculations were obtained using the temperature values for rod rolling obtained by the “Phantom Roll” method. Investigations were carried out for four different starting mean rolling temperatures between 900-1200°C, and four different rolling strain rates of 0.8, 0.4, 1.2, and 1.6s<sup>-1</sup>. Results obtained showed that for all cases, rolling in grooved rolls required more power (higher load) compared to rolling in flat rolls. Loads were higher for lower rolling temperatures for both flat rolls or grooved rolls. An increase in rolling speed also corresponded to an increase in load for both grooved and flat rolls. Straight-line equations fitted load against log<sub>10</sub>Z (where Z is Zener-Hollomon’s Parameter) at temperatures of 988°C, 1094°C, and 1095°C while two straight lines fitted the highest temperature of 1191°C in checking the combined effect of temperature and strain rate on load. This abnormal behavior is probably due to strain localization in two distinct zones caused by re-crystallization and incomplete recovery during working at the highest temperature of 1191°C.

(Keywords: simulation, phantom roll method, load, flat, grooved)

## INTRODUCTION

The “Phantom Roll” method allows the possibility of ignoring the temperature calculation in the roll while reasonable accuracy is maintained. It also makes it possible to save the computer calculation in the roll by assuming a parabolic temperature distribution. This method saves considerable computer time and memory

(Oseghale, 1997; Aiyedun et al., 2008). The ratio of the surface temperature change of slab and roll is obtained as a function of the thermal properties, the initial surface temperature of the slab and the roll, and the instantaneous slab surface temperature.

This concept was extended to rod rolling for both experimental and industrial rod rolling. The heat transfer coefficient (C) of 35-50kw/m<sup>2</sup>/°K was obtained from experimental values (Kawai, 1985). Values of up to C = 100kw/m<sup>2</sup>/°K were obtained for laboratory rod rolling while values of up to C = 200kw/m<sup>2</sup>/°K were reported for industrial rod rolling (Harding, 1976).

A lot of computer simulation models have been reported in the past in flat rolling, mainly for load calculations, to design mills at the maximum energy consumption (Kawai, 1985). Different assumptions were made for simplicity and the finite difference method was most commonly employed.

Kawai (1985) developed a computer simulation model which predicts temperature and micro structural changes for rod rolling of mild steel and medium carbon steel.

Aiyedun (1984) in his work made a comparison between the theoretical load and torque to that obtained experimentally using HC SS316 steel slab at low reduction and low strain rate (0.08-1.5s<sup>-1</sup>) by hot rolling the steel at different temperature using the modified. Leduc’s program which uses the Sim’s sticking friction approach. He observed that there was excessive load and torque in comparison with values obtained by normal rolling practice at low strain rates and low reduction for flat rolling. Similar conclusions have also been drawn through computer simulations using other approaches such as the Hot Rolling

Bland and Ford approach (Alamu and Aiyedun, 2003; Alamu et al., 2007)

Oseghale (1997) expanded the 'phantom roll' method to take care of load and torque calculations by neglecting the effect of roll flattening or deformation in the near surface region of the rolls. He also, in addition to the assumptions made by Kawai, assumed that a two dimensional deformation of metal (carbon manganese steel) during reduction.

For a C-Mn steel billet of size 125mm square rolled to 16mm diameter rod using 17 sequential passes, the following assumptions were used for simplification:

1. Water cooling for the material such as descaler and roll cooling systems were neglected.
2. Air cooling conditions were taken to be the same as in the laboratory although a lower cooling rate is probable due to the obstruction of the radiation by the trough between stands.
3. The roll radii and roll gaps were taken to be the same for all stands.

4. A two high laboratory mill with 254mm diameter grooved rolls was used for the rod rolling.
5. The shape of all grooves was round and varies from 254mm to 9.54mm.
6. Heat transfer coefficient (C) was taken to be 100kw/m<sup>2</sup>/°K initially and was increased inversely in proportion to the bar radius as rolling proceeded (since time between passes became very short later).
7. Mills that reduced round to oval before feeding into the mill that reduced the oval to round was a 50T, 2-High mill with 139mm diameter rolls.
8. The bar rotation about its longitudinal axis after each pass is taken at 90° (Cohrell, 1975; Raymond, 1983; Qamar, Beckley and Lewis, 1980).

The chemical composition of the steel employed is given in Table 1.

**Table 1:** Chemical Composition of the Steel Employed (Kawai, 1985).

Element	Amount (wt%)			Accuracy (wt%)	Method
	Material (1)	Material (2)	Material (3)		
C	0.47	0.37	0.40	0.01	L
Mn	0.72	0.63	0.70	0.02	Q
Si	0.20	0.20	0.23	0.02	Q
Al	0.005	0.047	0.039	0.003	Q
S	0.017	0.027	0.032	0.001	L
P	0.010	0.010	0.011	0.002	Q
Cr	0.18	0.11	0.25	0.02	Q
Ni	0.10	0.10	0.17	0.02	Q
N	0.0103	0.0068	0.0112	0.0003	L
Sn	0.016	0.010	0.017	0.003	Q
Cu	0.09	0.12	0.13	0.02	Q
Mo	0.02	0.02	0.06	0.02	Q
V	< 0.02	< 0.02	< 0.02	-	Q
Nb	< 0.02	< 0.02	< 0.02	-	Q
Ti	< 0.02	< 0.02	< 0.02	-	Q
Co	< 0.02	< 0.02	< 0.02	-	Q

Note 1: Material (1) and (2) are round bars for temperature measurement and Material (3) is flat bar for plane strain compression test.

Note 2: For Method L – Leco equipment model CS244 carbon sulphur analyzer  
Q – Quantometer.

## MATERIALS AND METHODS

### Mathematical Modeling

This is based on Table 2 which stipulates the conditions for rod rolling simulation from 125mm square billet to 16mm diameter rod (Kawai, 1985). The mathematical model used for the simulation is presented below:

$$\text{Rolling load, } P = F_d \cdot K_{wi} \quad (1)$$

$$F_d = b_m \cdot l_d \quad (2)$$

$K_{wi}^1$  can be used instead of  $K_{wi}$ , where

$K_{wi}^1$  = standard rolling deformation resistance of the rolled stock when only R, t,  $h_1/d$  are variables.

An analytical expression was derived which approximates very closely the Siebel's graphical function:

$$K_w^1 = f(R, t, h_1/d) \quad (3)$$

$$K_{wi}^1 = K \exp \alpha \quad (3)$$

$$\alpha = f(t, h_1/d) \quad (4)$$

$$\alpha = m.a.n.y \quad (4)$$

For conditions different from the predicted standard one, a number of correction factors are introduced and equation (3) becomes:

$$K_{wi} = (K \exp \alpha) a_1 a_2 a_3 a_4 a_5 \quad (5)$$

Where  $a_1, a_2, a_3, a_4$  and  $a_5$  are defined as follows:

$a_1$ : effect of relative rolling speed, (plotted as Figure 1) (Izzo, 1974).

$a_2$ : Tselikov's effect of the outer zones: for rolling of flats in free spread conditions (including blooming, slabbing, and roughing mills edging passes):  $a_2$  can be found as a function of  $l_d/h_m$  (Tselikov, 1967). See Figure 2 of Izzo, H.F. (1974).

$a_3$ : effect of form factor: assumed 1 for rolling in grooves; for rolling in flats, ( $a_3$  is plotted as Figure 3 a function of  $b_o/h_o \approx \delta$ ) (Izzo, 1974).

$a_4$ : effect of roll material, plotted as a function of the roll surface structure and HSC number. (HSC – roll surface hardness) (Figure 4) (Izzo, 1974).

$a_5$ : effect of chemical composition of rolled stock: for carbon steels, it is plotted as a function of  $h_1/d$ , KEM and t with:

$$KEM = \frac{4.2 + C + Mn + 0.3Cr}{4.77} \quad (6)$$

where C, Mn, and Cr are the percentage content of carbon, manganese and chromium (Figure 6) (Izzo, 1974).

In order to obtain Equations (3), (4), and (5), the following mathematical specifications are used:

Mathematical Specifications for Equations (3) and (4):

$$\text{SIGMA} = 100h_1/d \quad (7)$$

$$B = 3 + 0.350R \quad (8)$$

$$C = 10 + 0.025R \quad (9)$$

$$K = \frac{B}{\text{SIGMA}} + C \quad (10)$$

K and  $\exp \alpha$  are obtained as a function of  $h_1/d$ . (See Figure 5) (Izzo, 1974).

$$m = 1.797/(\text{SIGMA} 0.12 - 0.517) \quad (11)$$

$$a = (1000 - t)/1000 \quad (12)$$

$$n = 1 \text{ for } \text{SIGMA} \geq 1.2 \quad (13a)$$

$$n = (t/2000 + 0.35) + (0.65 - t/2000) \sin(300 \text{SIGMA} - 270) \text{ for } 1.2 > \text{SIGMA} > 0.6 \quad (13b)$$

$$n = t/1000 - 0.3 \text{ for } \text{SIGMA} \leq 0.6 \quad (13c)$$










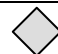
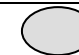
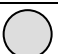

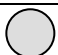




$$y = 1.5 \left( \frac{1100 - t}{458} \right)^{\frac{900 - t}{243.5}} - 1.8(\text{SIGMA} + 2)^{\frac{t - 1000}{100}}$$

$$\text{for } t < 1000 \quad (14a)$$

$$y = 1 \text{ for } 1000 \leq t \leq 1100 \quad (14b)$$

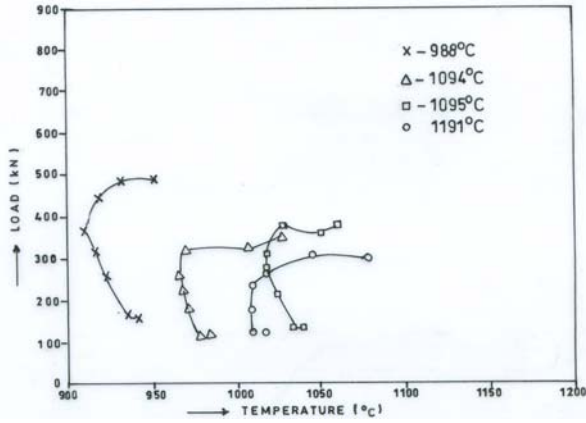
$$y = 1.6 \left( \frac{t - 1000}{426.5} \right)^{\frac{t - 1200}{127.3}} - 4.0(\text{SIGMA} + 4)^{\frac{1100 - t}{100}} \text{ for } t > 1100 \quad (14c)$$

**Table 2:** Conditions for Rod Rolling Simulation from 125mm square billet to 16mm diameter rod.  
(AFTER R. KAWAI)

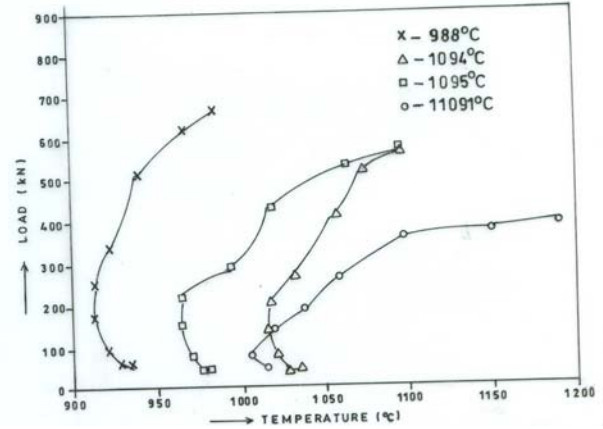
Pass No Furnace	Shape	Red.	E. Radius (mm)	$F_G$	Dist.(m)	V(m/s)	T(s)	$\Sigma t$ (s)
1			70.01	1.13	1	0.216	4.6	
		0.28						4.6
2			61.50	1.15	5	0.279	18.0	
		0.28						22.6
3			54.02	1.06	5	0.362	13.8	
		0.28						36.4
4			47.45	1	5	0.470	10.6	
		0.28						47.0
5			41.67	1.06	5	0.609	8.2	
		0.28						55.2
6			36.60	1.13	5	0.789	6.3	
		0.28						61.5
7			32.15	1.06	5	1.02	4.9	
		0.28						66.4
8			28.24	1.13	15	1.33	11.3	
		0.28						66.70
9			24.80	1.06	4	1.72	2.33	
		0.28						80.03
10			21.79	1.13	4	2.23	1.79	
		0.28						81.82
11			19.14	1.06	4	2.89	1.38	
		0.28						83.20
12			16.81	1	4	3.74	1.07	
		0.28						84.27
13			14.76	1.06	4	4.85	0.82	
		0.28						85.09
14			12.97	1	4	6.29	0.64	
		0.28						85.73
15			11.39	1.06	4	8.15	0.49	
		0.28						86.22
16			10.01	1	15	10.56	1.42	
		0.20						87.64
17			8.95	1.06	3	13.2	0.23	
		0.20						87.87
Stop			8.0	1		16.5	2.13	
								90.00

Red: Reduction  
 $F_G$ : Geometry Factor  
V: Rolling Velocity  
 $\Sigma t$ : Accumulated time

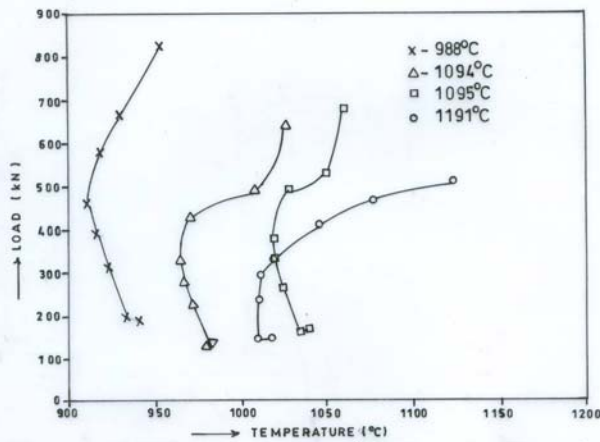
E. Radius: Equivalent Radius  
Dist.: Distance between rolling stands  
t: Time



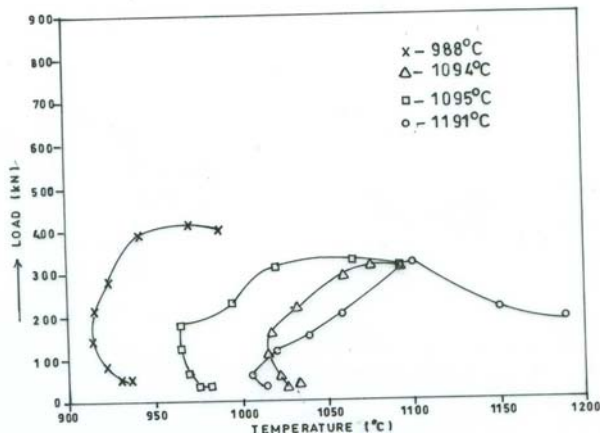
**Figure 1:** Load vs. Temperature for Rod Rolling using Grooved Rolls at 0.5 times Initial Rolling velocity for Temperatures of 988, 1094, 1095, and 1191°C.



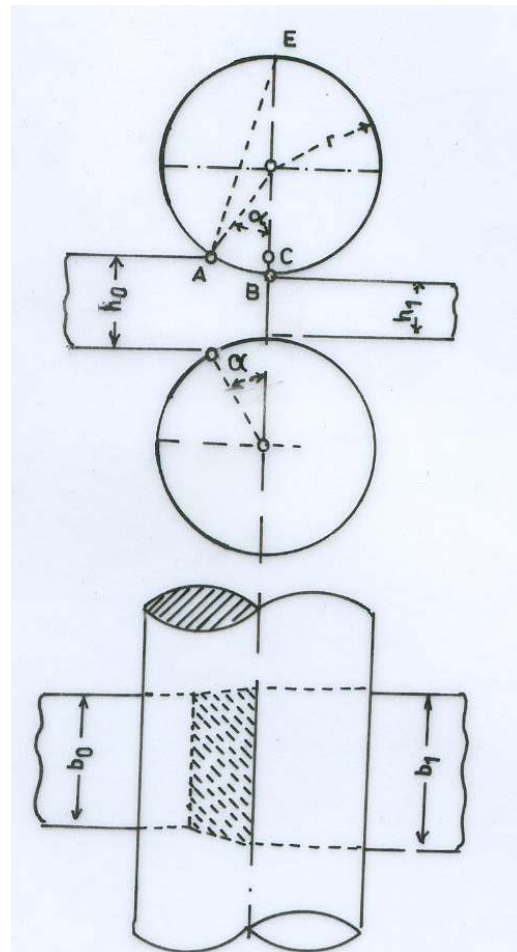
**Figure 4:** Load vs. Temperature for Rod Rolling using Flat Rolls at 2.0 times Initial Rolling velocity for Temperatures of 988, 1094, 1095, and 1191°C.



**Figure 2:** Load vs. Temperature for Rod Rolling using Grooved Rolls at 2.0 times Initial Rolling velocity for Temperatures of 988, 1094, 1095, and 1191°C.



**Figure 3:** Load vs. Temperature for Rod Rolling using Flat Rolls at 0.5 times Initial Rolling velocity for Temperatures of 988, 1094, 1095, and 1191°C.



**Figure 5:** Area of Contact between Rolled Material and Rolls.

Mathematical specifications for Equation (5)  
Coefficients  $a_1$  (rolling speed):

$$\text{THETA} = 0.142 + 0.023 \left( \frac{t - 800}{200} \right)^{2.34} \quad (15a)$$

$$\text{TAU} = 1.5 - v/d \quad (15b)$$

$$a_1 = 1 + \text{THETA} \ln(1 - \text{TAU}) \text{ for } v/d \geq 1.5 \quad (16a)$$

$$a_1 = 1 - \text{THETA} \cdot \text{TAU} - 0.257 \text{TAU}^3 + 0.0547 \text{TAU}^5 \text{ for } v/d < 1.5 \quad (16b)$$

Coefficient  $a_2$  (outer zones or additional friction):

$$a_2 = 1 \text{ for } l_d/h_m \geq 1 \quad (\text{FR}) \quad (17a)$$

$$a_2 = (l_d/h_m)^{-0.4} \text{ for } l_d/h_m < 1 \quad (\text{FR}) \quad (17b)$$

$$a_2 = 1.003 \leq a_2 \leq 1.300 (\text{BR}) \quad (17c)$$

Coefficient  $a_3$  (form factor)  
DELTA =  $b_o/h_o$  (18a)

$$A = \ln \text{DELTA} \text{ RHO} = \left( \frac{60 - R}{100} \right)^3 \quad (18b)$$

$$a_3 = 0.797 - \text{RHO} \text{ for } A \leq 0 \quad (\text{FR}) \quad (19a)$$

$$a_3 = 0.797 - \text{RHO} + 0.247A \text{ for } 0 < A < 1 \quad (\text{FR}) \quad (19b)$$

$$a_3 = 1.037 - \text{RHO} + 0.007A \text{ for } A \geq 1 \quad (\text{FR}) \quad (19c)$$

$$a_3 = 1 \quad (\text{BR})$$

Coefficient  $a_4$  (roll surface hardness and structure):

KSC = Roll surface structure;

HSC = Roll surface hardness shore C number

KSC = 0.000 for steel and steelbase  
= 0.001 for Nodular and Pearlitic Cast Iron  
= 0.002 for Nodular Martensitic Cast Iron  
= 0.003 for CC and IC Cast Iron

$$a_4 = 1 - 0.05(\text{HSC} - 40) (0.0001 R + \text{KSC}) \quad (20)$$

Coefficient  $a_5$  (grade of rolled steel):

$$\text{KEM} = \frac{4.2 + C + \text{Mn} + 0.3\text{Cr}}{4.77} \quad (21)$$

$$\text{OMEGA} = \frac{1 - (2 - \text{KEM})^{17}}{2} \quad (22)$$

$$a_5 = 1 + \frac{1200 - t}{220} \text{OMEGA} (1 - 0.335 \ln \text{SIGMA}) \text{ for } \text{SIGMA} \leq 14 \quad (23a)$$

$$a_5 = 1 + \frac{1200 - t}{220} \text{OMEGA} (251/\text{SIGMA}^{2.91}) \text{ for } \text{SIGMA} > 14 \quad (23b)$$

### Load Calculation

$$\text{Rolling Load } P = F_d \cdot K_{wi} \quad (24)$$

$$\text{where } F_d = b_m \cdot L_d \quad (25)$$

$L_d$  = projected contact length

See Figure 5 for relationship between  $b_m$  and  $L_d$ .  
According to Tselikov (1967),

i. For a square rolled from oval,  $F = 0.75b_1[r_1(h_0 - h_1)]^{1/2} \quad (26)$

ii. For an oval rolled from a square,  $F = 0.54(b_0 + b_1)[r_1(h_0 - h_1)]^{1/2} \quad (27)$

iii. For a rhombus or square rolled from a rhombus,  $F = 0.67b_1[r_1(h_0 - h_1)]^{1/2} \quad (28)$

### Calculation of Zener-Hollomon's Parameter (Z)

$$Z = \bar{\epsilon} \exp(Q/R_g \cdot T) \quad (29)$$

= 270kj/mole:  $R_g$   
= 8.13j/°K: T = Absolute Temperature

$$\bar{\epsilon} = 1.08V/(R \cdot \Delta h)^{0.5} \left[ (\Delta h)^2 / h_1 h_2 \right]^{0.25} \left[ \ln(h_1/h_2)^{0.45} \right] \quad (30)$$

### Calculation of Graph Equations

$$\text{Load } (P) = A \log_{10} Z + B \quad (31)$$

with A and B as constants which were obtained from curve fitting of load vs  $\log_{10} Z$  for various temperatures for both grooved and flat rolls.

From Figures 6 and 7 (Load versus  $\log_{10} Z$  for rod rolling using grooved rolls and flat rolls respectively) the following equations were obtained:

$$P = -166.4 \log_{10} Z + 3144 \quad (32)$$

$$P = -100 \log_{10} Z + 1780 \quad (33)$$

$$P = -160 \log_{10} Z + 2665.6 \quad (34)$$

$$P = -160 \log_{10} Z + 2665.6 \quad (35a)$$

$$P = -17.24 \log_{10} Z + 187.9 \quad (35b)$$

for temperatures 988, 1094, 1095, and 1191°C, respectively.

$$P = -220 \log_{10} Z + 3876 \quad (36)$$

$$P = -125 \log_{10} Z + 2062.5 \quad (37)$$

$$P = -133.3 \log_{10} Z + 2230 \quad (38)$$

$$P = -95.24 \log_{10} Z + 1559.3 \quad (39a)$$

$$P = -3.64 \log_{10} Z + 353.1 \quad (39b)$$

for temperatures 988, 1094, 1095, and 1191°C respectively.

## RESULT AND DISCUSSIONS

A typical printout of the simulation result is shown on Table 4 for a rolling temperature of 1094°C, and rolling speed of 2V, 2 times initial rolling speed (i.e., a strain rate of  $1.6s^{-1}$ , based on input data for 17 passes in Table 3).

Results obtained for 4 different starting mean temperatures of 988, 1094.5, 1095.5 and 1191°C; four rolling speeds of 0.5, 1.0, 1.5 and 2.0 times the initial speed (i.e., strain rates of 0.4, 0.8, 1.2 and  $1.6s^{-1}$ , respectively) were investigated. According to some earlier work, Kawai (1985) obtained that increasing rolling speed by 1.5 times increased the final rolling temperature by 65°C and equally increased the final grain size considerably hence he concluded that rolling speed could be used to control the rolling operations.

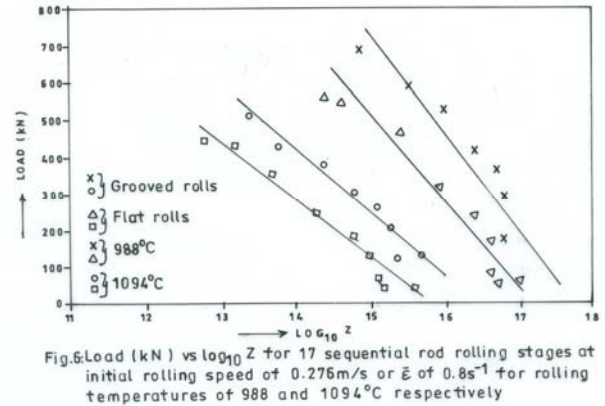


Figure 6: Load versus  $\log_{10} Z$  for Rolling Temperatures of 988 and 1094°C.

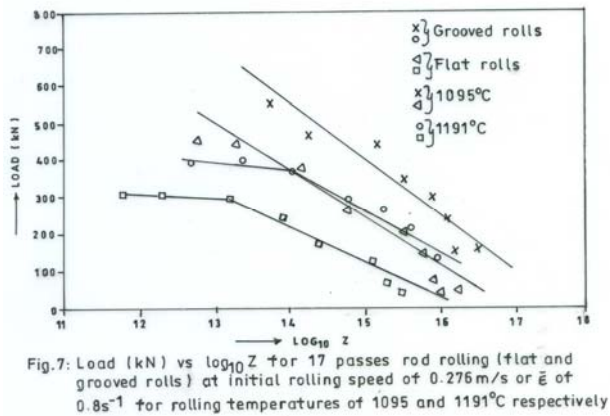


Figure 6: Load versus  $\log_{10} Z$  for Rolling Temperatures of 1095 and 1191°C.

From results obtained in this work, for all cases, rolling in grooved rolls required more power as evidenced by higher loads observed for grooved rolls compared with the flat rolls. Loads in grooved rolls were higher than those in flat rolls by about 70kN at 1094°C and about a 100kN at 988°C. This is possibly due to the following reasons:

1. For rolling in grooved rolls, the area of contact between rolls and metal increases towards exit and not constant as in flat rolls. Since load is a function of contact area, this could account for the difference.
2. Frictional effect due to side wall of the grooved rolls is greater because of the greater contact area.

**Table 3:** Typical Input Data for 17 passes Sectional Rolling in Grooved and Flat Rolls. Rolling Temperatures,  $T = 1094.5^{\circ}\text{C}$  and a 2.0 times initial rolling speed (i.e.  $\bar{\epsilon} = 1.6\text{s}^{-1}$ ).

H0	H1	D	T	V1	KX1	KX2	B0	B1
140.2	125.3	278.0	1074.5	0.552	1	1	140.2	123.0
125.3	110.3	278.0	1074.5	0.724	1	1	123.0	108.0
110.3	97.0	508.0	1060.9	0.940	0	2	108.0	94.9
97.0	83.3	278.0	1060.9	1.218	1	1	94.9	83.3
83.3	75.3	508.0	1050.0	1.578	0	3	83.3	73.2
75.3	66.6	278.0	1031.8	2.04	1	1	73.2	64.3
67.0	58.6	508.0	1027.3	2.66	0	3	64.3	56.5
58.6	51.9	278.0	1017.3	3.44	1	1	56.5	49.6
51.9	45.7	508.0	1017.3	4.46	0	3	49.6	43.6
45.7	40.54	278.0	1017.3	5.38	1	1	43.6	38.3
40.5	33.63	508.0	108.2	7.48	0	2	38.3	33.6
33.6	31.7	278.0	1022.7	9.36	1	1	33.6	29.6
31.7	25.94	508.0	1025.0	15.58	0	2	29.6	25.9
25.9	24.9	278.0	1029.6	16.3	1	1	25.9	22.8
24.9	22.0	508.0	1034.1	21.12	0	2	22.8	20.0
22.0	20.0	278.0	1034.1	26.4	1	1	20.0	17.9
20.0	16.0	508.0	1040.0	33.0	0	2	17.9	16.0

**Table 4:** Results Obtained from the Simulation of Rod Rolling for an Initial Mean Rolling Temperature of  $1094^{\circ}\text{C}$  and a 2.0 times Initial Rolling Speed (i.e.  $\bar{\epsilon} = 1.6\text{s}^{-1}$ ).

(a) For Rolling in Grooved Rolls.

	Given temp. ( $^{\circ}\text{C}$ )	Load (kN)	Specific Pressure ( $\text{N}/\text{mm}^2$ )	$\text{Log}_{10}Z$	Strain Rate ( $\text{s}^{-1}$ )
1	1027	632	94	13.7	2.5
2	1007	485	109	14.1	4.3
3	970	422	130	14.7	9.2
4	964	325	150	15.1	17.1
5	968	280	174	15.4	39.2
6	973	223	199	15.7	95.7
7	979	131	199	15.7	115.2
8	983	135	239	15.9	269.7

(b) For Rolling in Flat Rolls.

	Given temp. ( $^{\circ}\text{C}$ )	Load (kN)	Specific Pressure ( $\text{N}/\text{mm}^2$ )	$\text{Log}_{10}Z$	Strain Rate ( $\text{s}^{-1}$ )
1	1094	555	93	13.1	1.6
2	1075	516	98	13.5	2.4
3	1061	402	104	14.0	5.0
4	1032	272	113	14.6	8.7
5	1017	195	120	15.1	16.5
6	1017	136	124	15.3	28.9
7	1023	70	13	15.4	41.9
8	1030	43	147	15.5	70.3
9	1034	44	141	15.9	185.9

Values of load were higher for lower temperatures and lower for higher temperatures. Also an increase in speed corresponded to an increase in mean specific pressure and hence in load for the same starting temperature.

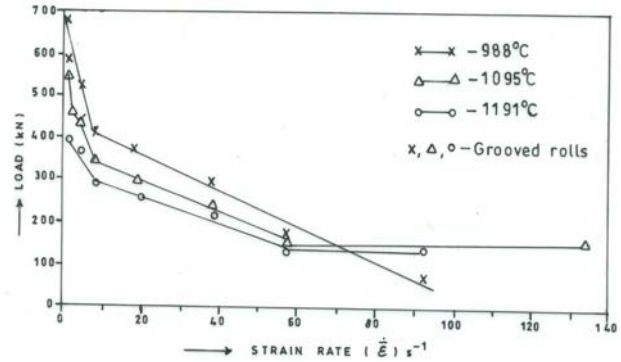
For the plot of load against temperature, hyperbolic curves were obtained both for grooved rolling and flat rolling (Figures 1-4). As the velocity increased, the curves tend to be less hyperbolic and conic in shape for all four temperatures. During working, the load is high at first during deformation due to the rate of hardening which is greater than the rate softening associated with recovery. Being at elevated temperature, further softening takes place either by continuation of recovery or by re-crystallization. Hence even with a rise in temperature towards end of rolling, the load reduced without a corresponding reduction in temperature thus explaining the conic shape of the curves.

To check the combined effect of temperature and rolling speed on load, the Zener-Hollomon parameter ( $Z$ ) which combined their effect was calculated and the plot of load against  $\log_{10} Z$  were obtained for grooved and for flat rolling.

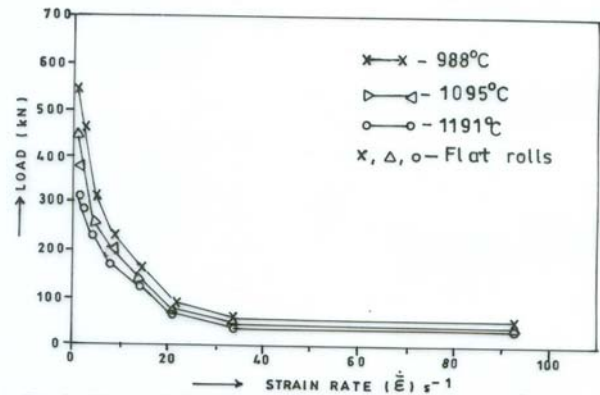
These were fitted with straight lines for the starting temperatures of 988, 1094, and 1095°C while a peculiar variation was observed for the highest temperature of 1191°C. Two sets of straight line equations fitted these points. This trend was general for the various speeds investigated (see Figures 6 and 7).

The reason for this abnormal behavior could be that re-crystallization and hence recovery never fully took place during its working thereby resulting in strain localization in two distinct zones resulting in the two straight lines used in fitting the points (see Figure 7).

Load versus rolling strain rate were plotted for rolling temperatures of 988, 1095, and 1191°C (see Figures 8 and 9, respectively). From these set of results it can be seen that for grooved rolls, loads were high and close for the first few (2-3) rolls while they were more scattered and pronounced for the remaining rolls whereas for the flat rolls, for various temperatures of rolling the load were within the same narrow bands for all rolling strain rates.



**Figure 8:** Plot of Load versus Strain Rate for Rod Rolling Using Grooved Rolls at Initial Speed of 0.276m/s for Roll Temperatures of 988, 1095, and 1191°C.



**Figure 8:** Plot of Load versus Strain Rate for Rod Rolling Using Flat Rolls at Initial Speed of 0.276m/s for Roll Temperatures of 988, 1095, and 1191°C.

## CONCLUSION

1. Rolling in grooved rolls require more power as evidenced by the higher values of load observed for the grooved rolls compared to the flat rolls.
2. Loads are higher for lower temperatures as shown in the data table above for both flat rolls and grooved rolls.
3. An increase in rolling speed corresponds to an increase in mean specific pressure and hence loads for the same starting temperature for the grooved rolls or flat rolls.
4. Plots of load versus temperature gave hyperbolic curves that are convex in nature.

The convex nature of these curves reduces with increase in the rolling velocity.

5. Straight line equations fitted load against  $\log_{10}Z$  for temperatures of 988, 1094 and 1095°C while two straight lines fitted the highest temperature of 1191°C for the various speeds.
6. In plots of load versus rolling strain rates (Figures 8 and 9), it can be seen that for grooved rolls, the loads were high and close for the first few 2-3 rolls while they were more scattered and pronounced for the remaining rolls whereas for the flat rolls, for various temperatures of rolling, the loads were within the same narrow band for all rolling strain rates.

## NOTATIONS

- P: Rolling Load (kg or N)
- T: Rolling Torque (kN-m) or rolling temperature, (°C) or absolute temperature, °K.
- $b_0, h_0$ : Initial stock width, mm, entry stock thickness, mm
- $b_1, h_1$ : Final stock width, mm; exit stock thickness, mm
- $b_m$ :  $(b_0 + b_1)/2$  – average stock width, mm
- d: roll diameter, mm
- $\alpha$ : Angle of contact or exponential function which depends on  $t_1, h_1/d$
- d: Roll diameter, mm
- $\bar{\epsilon}$ : Strain rate, ( $s^{-1}$ )
- $h_m$ :  $(h_0 + h_1)/2$ , average stock thickness, mm
- $\Delta h$ :  $h_0 - h_1$ , reduction in thickness, mm
- $l_d$ :  $(\Delta h \cdot d/2)^{1/2}$ , projected contact length, mm
- r:  $(h_0 - h_1)/h_0$ , fractional reduction or roll radius
- R: 100r, percentage reduction, %

- t, T: Rolling temperature, °C
- v: Rolling speed, m/s. or peripheral velocity of rolls
- BR: Bar rolling
- FR: Flat rolling
- $F_d$ : Projected contact area,  $mm^2$
- $R_g$ : Gas constant = 8.13j/°K
- $K_{wi}$ : Mean rolling pressure,  $kg/mm^2$
- K: Yield strength of the rolled stock at a temperature of 1000°C
- KSC: Roll surface structure
- HSC: Roll surface hardness
- SRC: (Standard Rolling Condition) yield strength for following rolling conditions:
1. Relative rolling speed (v/d) between 1-2 $s^{-1}$ .
  2. Plain barreled rolls
  3. Form factor ( $b_0/h_0$ ) between 2 – 4
  4. Steel rolls with surface hardness about 40 shore C
  5. Rolled stock with carbon content about 0.1%
- KEM: Function of the rolled steel composition

## REFERENCES

1. Aiyedun, P.O., Igbudu, O.S. and Bolaji, B.O. 2008. "Simulation of Load during Rod Rolling Of HC SS316 at Low Strain Rate". Paper presented at the Second International Conference on Engineering Research & Development. *Innovations* (ICER & D 2008). University of Benin, Benin City, Nigeria 15 - 17 April 2008.
2. Aiyedun, P.O. 1984. "A Study of Loads and Torque for Light Reduction in Hot Flat Rolling at Low Strain Rates". Ph.D. Thesis. University of Sheffield, UK.
3. Alamu, O.J. and Aiyedun, P.O. 2003. "A Comparison of Temperature Gradient in Hot Rolling at Low and High Strain Rates". *J. Sci. Engr. Tech.* 10(1):4644 – 4654.

4. Alamu, O.J., Aiyedun, P.O., Kareem, A. and Waheed, M.A. 2007. "Effect of AISI 316 Stainless Steel Geometry on Temperature Distribution During Hot Rolling at High Reduction". In: *Advanced Materials Research -Advances in Materials and System Technologies*. Vols. 18-19, pp. 195-200. Trans Tech Publications Ltd.: Switzerland.
5. Cohrell, A. 1975. *An Introduction to Metallurgy. 2nd edition*. E. Arnold, Pub.: New York, NY.
6. Harding, R.A. 1976. "Temperature and Structural Changes during Hot Rolling". Ph.D. Thesis. University of Sheffield, Sheffield, UK.
7. Izzo, H.F. 1974. "Report on a Hot Rolling Formula", *JISI*. 47(1):101.
8. Kawai, R. 1985. "Simulation of Rod Rolling of Carbon Manganese Steel". M. Phil. Thesis, Department of Metallurgy, University of Sheffield, Sheffield, UK.
9. Oseghale, L.E.E. 1997. "Simulation of Load and Torque during Rod Rolling using the 'Phantom Roll' Method". M.Sc. Thesis, Mechanical Engineering Department, University of Ibadan, Ibadan.
10. Parrish, A. 1973. *Mechanical Engineers Reference Book*. Butterworth & Co. Ltd., London, UK.
11. Qamar, K.H., Buckley, G.W., and Lewis, M. 1980. "Computer Programmed Speeds Roll-torque Data Calculation". *JISI*. 53(1):29-37.
12. Raymond, A.H. 1983. *Engineering Metallurgy. 5th & 6th Edition*. ELBS: London, UK.
13. Tselikov, A. 1967. *Stress and Strain in Metal Rolling. 2nd Edition*. Mir. Publishers: Moscow, Russia.

## ABOUT THE AUTHORS

**Prof. Peter Olaitan Aiyedun** is a Professor of Mechanical Engineering, University of Agriculture, Abeokuta, Nigeria. He is a Chartered Engineer and a Fellow of the Nigeria Society of Engineers. He holds a Ph.D. degree in Mechanical Engineering. His research interests are in the area of production, materials, nuclear and environmental engineering.

**Oseghale, L.E.** is a graduate of the Ahmadu Bello University, Zaria, Nigeria. He holds M.Sc. degree in Mechanical Engineering from the University of Ibadan, Nigeria. He is currently a

staff of Chevron. His research interest is in materials engineering.

**Dr. Alamu, Oguntola Jelil** is the current Head of Department of Mechanical Engineering, University of Agriculture, Abeokuta, Nigeria. He holds a Ph.D. degree in Mechanical Engineering. His research interests are in renewable energy, thermofluids and materials science & engineering.

## SUGGESTED CITATION

Aiyedun, P.O., L.E. Oseghale, and O.J. Alamu. 2009. "Simulation of Load Bearing Rod Rolling of Carbon-Manganese Steel Using the "Phantom Roll" Method". *Pacific Journal of Science and Technology*. 10(1):4-14.



[Pacific Journal of Science and Technology](http://www.akamaiuniversity.us/PJST.htm)